Quantification of interaction and topological parameters of polyisoprene star polymers under good solvent conditions

Durgesh K. Rai, Gregory Beaucage, Kedar Ratkanthwar, Peter Beaucage, Ramnath Ramachandran, and Nikos Hadjichristidis

Phys. Rev. E **93**, 052501 — Published 5 May 2016

DOI: 10.1103/PhysRevE.93.052501

Quantification of interaction and topological parameters of polyisoprene star polymers under good solvent conditions

Durgesh K Rai[1*], Gregory Beaucage[2**], Kedar Ratkanthwar[3,4], Peter Beaucage[5], Ramnath Ramachandran[6], Nikos Hadjichristidis[3,4]

[1]*Biology and Soft Matter Division, Oak Ridge National Laboratory, Oak Ridge, TN-37831, USA,*

[2]*Materials Science and Engineering, University of Cincinnati, Cincinnati, OH-45221, USA*

[3]*Department of Chemistry, University of Athens, Panepistimiopolis, Zografou, 15771, Athens, Greece*

[4]*Division of Physical Sciences and Engineering, KAUST Catalysis Center, King Abdullah University of Science and Technology (KAUST), Thuwal, Saudi Arabia*

[5]*Department of Materials Science and Engineering, Cornell University, Ithaca, NY 14853*

[6]*Procter & Gamble, 1 P&G Plaza, Cincinnati, OH-45202, USA*

* Oak Ridge National Laboratory; PO Box 2008; MS-6454; Oak Ridge, TN 37831, USA; Email: raidk@ornl.gov, preferred email: raidurgesh@hotmail.com

** University of Cincinnati, 492 Rhodes Hall, Cincinnati, OH-45221, USA; E-mail: beaucag@uc.edu, preferred email: gbeaucage@gmail.com

ABSTRACT

Mass fractal scaling, reflected in the mass fractal dimension d_f, is independently impacted by topology, reflected in the connectivity dimension c, and by tortuosity, reflected in the minimum dimension $d_{\min}$. The mass fractal dimension is related to these other dimensions by $d_f = cd_{\min}$. Branched fractal structures have a higher mass-fractal dimension compared to linear structures due to a higher c, and extended structures have a lower dimension compared to convoluted self-avoiding and Gaussian walks due to a lower $d_{\min}$. It is found, in this work, that macromolecules in thermodynamic equilibrium display a fixed mass-fractal dimension, d_f, under good solvent conditions, regardless of chain topology. These equilibrium structures accommodate changes in chain topology such as branching, c, by a decrease in chain tortuosity, $d_{\min}$. Symmetric star polymers are used to understand the structure of complex macromolecular topologies. A recently published hybrid Unified scattering function, accounts for inter-arm correlations in symmetric star polymers along with polymer-solvent interaction for chains of arbitrary scaling dimension. Dilute solutions of linear, 3-arm and 6-arm polyisoprene stars are studied under good solvent conditions in deuterated *p*-xylene. Reduced chain tortuosity can be viewed as steric straightening of the arms. Steric effects for star topologies are quantified and it is found that steric straightening of arms is more significant for lower molecular weight arms. The observation of constant d_f is explained through a modification of Flory-Krigbaum theory for branched polymers.

INTRODUCTION

The physical properties of branched polymers are different from linear chains of comparable molecular weight [1-3]. Amongst various possible branched architectures, symmetric star polymers are one of the simplest topologies and have been widely studied from the perspective of synthesis, structure, properties and application [4-8]. Star polymers are branched macromolecules with all branches or "arms" emanating from a core. The presence of structural constraints, owing to the presence of a common branch point, leads to differences in chain conformation and thermodynamics in star polymers compared to their linear counterparts [9-15]. Moreover, the number and structure of arms have been found to have direct consequences on rheological properties of branched polymers [16-18].

Zimm and Stockmayer (Z&S) evaluated the radius of gyration, R_g^{star}, of a star polymer with f arms in dilute solution assuming that intra- and inter-arm spacings follow Gaussian statistics [11, 12],

$$R_g^{star} = R_g^{arm}\left(\frac{3f-2}{f}\right)^{\frac{1}{2}} \tag{1}$$

where, R_g^{arm} is the radius of gyration of a Gaussian linear chain in dilute solution with the mass of one arm. A notable result inferred from equation (1) is that the ratio, $R_g^{star} \big/ R_g^{arm}$ has a maximum limiting magnitude of $\sqrt{3}$ as, $f \to \infty$ under a Gaussian assumption. This result is rather meaningless since steric constraints would render the arms highly non-Gaussian at high f. Moreover, the results from the Gaussian approximation for stars may not hold under virtually any conditions since the intra-molecular excluded volume becomes more significant due to increase in segment-segment interactions near the branch point and the Gaussian assumption fails to recognize the singular nature of the branch point [19]. For stars with higher functionality, the arms of the star might behave as stiff chains with a limiting conformation of rigid straight arms for very high f. Assuming a limiting rigid straight arm configuration for stars, $R_g^{star} \big/ R_g^{arm} \sim \sqrt{z_{arm}}$, for $f \rightarrow \infty$, where z_{arm} is the mass associated with each arm and R_g^{arm} is assumed to be Gaussian. This is significantly larger than the prediction of equation (1) at large f.

Daoud & Cotton (D&C) and later Birshtein & Zhulina addressed the issue of minimization of the free energy due to intermolecular interactions by generalizing the de Gennes's scaling (blob) model for star polymers [12-14, 20]. The inter-arm repulsive interaction was minimized by assuming that equal segments of the arms are confined to growing spherical blobs that can fit into a cone as the arms extend away from the branch point (core). The star polymer adopts a conformation in which each of the f arms is constrained within a cone of solid angle $4\pi/f$ radiating from the branch point which leads to increases in the mean separation between the arms with the distance from the center [13, 19]. As per the D&C model, the star polymer is confined to shells of decreasing chain density. There is no scattering function associated with D&C model so it is difficult to directly verify this structural model. Under another widely used theory for the star polymers, the chain structure does not display core/shell morphology but it rather acquires a uniform chain density as per the Benoit's model for star polymers [21, 22]. The Benoit model assumes Gaussian conformation consistent with the Zimm and Stockmayer model but allows for inter-arm correlations that have been verified experimentally

The Daoud and Cotton, DC, model describes the conformation of a star polymer with f arms with l and v as the monomer length and excluded volume [13, 14, 20]. According to the DC model, a star polymer has a solid core of radius $r_2 \sim f^{1/2} l$, where the monomer concentration $\phi(r)$ is constant since $\phi(r) \sim M/V$ and for a 3-dimensional solid, $M \sim (r/l)^3$ and $V \sim (r/l)^3$. Thereafter, $\phi(r)$ varies as $(r/l)^{-1}$ between r_2 and r_1 which fits Gaussian scaling since for a Gaussian chains, $M \sim (r/l)^2$ and $V \sim (r/l)^3$ leading to $\phi(r) \sim (r/l)^{-1}$, where $r_1 \sim f^{1/2} v^{-1} l$. Finally, $\phi(r) \sim (r/l)^{-4/3}$ for $r > r_1$, which suggests good solvent scaling for larger distances from core since for a chain under good solvent condition, $M \sim (r/l)^{5/3}$ and $V \sim (r/l)^3$ leading to $\phi(r) \sim (r/l)^{-4/3}$. The modified Flory-Krigbaum model, presented below, predicts that $\phi(r) \sim (r/l)^{-4/3}$ irrespective of distance from core, similar to the Zimm-Stockmayer and Benoit models, with packing constraints accommodated by straightening out of the arms near the core. The Kuhn unit density is constant with good solvent scaling through out the star. The model follows the same scaling laws as the large distance prediction of the DC model.

For the "swollen region" [13] of the star, the DC model predicts,

$$R \sim f^{\frac{1}{5}} \left(\frac{z}{f} \right)^{\frac{3}{5}} V_C^{\frac{1}{5}} l_k \sim f^{-\frac{2}{5}} z^{\frac{3}{5}} V_C^{\frac{1}{5}} l_k \tag{2}$$

where, R is the chain end to end distance and V_C is the excluded volume per Kuhn unit of length l_k. $z = f z_{arm}$ is the total mass associated with all the f arms of the star polymer. On the other hand, for the "unswollen" region,

$$R \sim f^{\frac{1}{4}}\left(\frac{z}{f}\right)^{\frac{1}{2}} l_k \sim f^{-\frac{1}{4}} z^{\frac{1}{2}} l_k \tag{3}$$

For comparison, using Zimm and Stockmayer's equation (1), Orofino predicts the size of symmetric star polymers to be [11, 23, 24],

$$R \sim \left(\frac{3f-2}{f}\right)^{\frac{1}{2}}\left(\frac{z}{f}\right)^{\frac{1}{2}} l_k \sim \frac{(3f-2)^{\frac{1}{2}}}{f} z^{\frac{1}{2}} l_k \tag{4}$$

for $\theta-$solvent conditions.

Modification of the Flory-Krigbaum Model for Star Polymers

Flory and Krigbaum [25-27] predicted that the expected mass-fractal dimension for a linear chain ($c=1$ defined below) in a good solvent is 5/3 ($d_{\min} = d_f = 5/3$ defined below). This is obtained by modification of the Gaussian chain probability function by a term reflecting self-avoidance resulting in the expression,

$$W(R) = kR^2 \exp\left(-\frac{3R^2}{2zl_k^2} - \frac{z^2 V_C}{2R^3}\right) \tag{5}$$

where k is a constant. The first term describes Gaussian scaling and the second term reflects excluded volume by considering the probability of one Kuhn unit being excluded by one of the other Kuhn units of the chain. Assuming that, due to symmetry, a linear chain of length $2\pi/f$ has the same size as a star of mass z if the two structures have the same degree of tortuosity reflected in $d_{\min}$, $(2\pi/f)$ substituted for z in equation (5). In the symmetric star V_C from the linear chain of length $2\pi/f$ is amplified by f. So fV_C substitutes for V_C,

$$W\left(R\right)=kR^2\exp\left(-\frac{3fR^2}{4zl_k^2}-\frac{\left(2z/f\right)^2 fV_C}{2R^3}\right)=kR^2\exp\left(-\frac{3fR^2}{4zl_k^2}-\frac{2z^2V_C}{fR^3}\right) \tag{6}$$

Equation (5) can be minimized to find the most likely chain end-to-end distance, R^*, ignoring higher order terms,

$$R^*=R_0^*\left(\frac{2z^{\frac{1}{2}}V_C}{l_k^3}\right)^{\frac{1}{5}}=kz^{\frac{3}{5}}V_C^{\frac{1}{5}}l_k^{\frac{2}{5}} \tag{7}$$

A similar minimization of equation (6) yields,

$$R^*=k\left(\frac{z}{f}\right)^{\frac{3}{5}}\left(fV_C\right)^{\frac{1}{5}}l_k^{\frac{2}{5}}=kf^{-\frac{2}{5}}z^{\frac{3}{5}}V_C^{\frac{1}{5}}l_k^{\frac{2}{5}} \tag{8}$$

Equation (8) predicts that d_f is independent of f since $R^*\sim z^{1/d_f}$, and that $d_f=5/3$ for macromolecules in good solvents regardless of topology. Equation (8) also predicts a dependence on functionality similar to that of DC model described by equation (2). It is expected that Gaussian chains will display a mass fractal dimension of 2 regardless of chain topology, as assumed by the DC and Zimm and Stockmayer models. For chains with a fixed mass fractal dimension and variable branch content the connectivity dimension will increase with branching, and since $d_{\min}=d_f/c$, a reduction in $d_{\min}$ and straightening out of the star arms is expected, as discussed below. Table 1 shows the three predictions for chain size from the ZS, DC and modified FK models.

SCALING MODEL FOR SYMMETRIC STAR POLYMERS

In this paper, a newly proposed method to analyze scattering from star polymers is used based on a scaling model that allows for study of steric chain extension as well as accounting for polymer-solvent interactions. The scaling approach quantifies the topological as well as thermodynamic parameters for different molecular weights for their linear, 3-arm and 6-arm polyisoprene stars under good solvent condition at 34.5 ˚C in deuterated *p*-xylene [28].

In the scaling model a macromolecular chain composed of z Kuhn units of length l_k [29] is considered. Figure 1 shows a 6-arm symmetric star polymer. The structure displays tortuosity in the chain path associated with a competition between thermal randomization of the chain structure, chain continuity and steric constraints. The structure also displays topological connectivity that is independent of these thermodynamic and steric constraints. These features can be distinguished by considering the average minimum path of p Kuhn units through the structure [30-32]. One possible minimum path is shown in units with dark borders in figure 1. In addition to an average minimum path, an average connectivity path of s Kuhn units composed of straight lines connecting the branch point and chain end-points is considered as shown by solid black lines in figure 1. In the case of symmetric star polymers, the minimum path is composed of two arms of the star polymer (dark units in figure 1). For a symmetric star polymer, the average minimum path, p, is given by,

$$p = 2\left(\frac{z}{f}\right) \tag{9}$$

In general, the minimum path, p, is related to the mass, z, through the connectivity dimension, c, which represents the mass fractal dimension for the connectivity path. On the other hand, the connectivity path of s is related to the mass through minimum dimension, $d_{\min}$, which represents the mass fractal dimension for the minimum path. Two pairs, $s:d_{\min}$ and $p:c$, work in tandem to represent the whole structure as a mutually conjugate set of parameters such that the mass, z, can be obtained by raising the connectivity path, s, to the minimum dimension, $d_{\min}$, or alternately, raising the minimum path, p, to the topological connectivity dimension, c, giving, [31, 33, 34]

$$z = p^{c} = s^{d_{\min}} \tag{10}$$

The connectivity dimension, *c*, quantifies the structural connections between the various arms of the polymer and is related to the fractal dimension, d_f, by [31],

$$d_f = c d_{\min} \tag{11}$$

c increases with increased branching or connectivity, while d_f increases with tortuosity in the chain. For a linear polymer chain, $d_{\min} = d_f$ and $c = 1$ while, for a completely connected regular object like a sphere or a collapsed coil, $d_f = c$ and $d_{\min} = 1$, since the minimum path becomes a straight line across the whole mass. For a chain under good solvent conditions, $d_{\min} = 5/3$ [31].

For symmetric stars, the mole fraction branch content (ϕ_{Br}) is given by [31],

$$\phi_{Br} = \frac{(z-p)}{z} = 1 - z^{-\left(1-\frac{1}{c}\right)} = \frac{(f-2)}{f} \tag{12}$$

where, $(z-p)$ represents the mass of the coil that does not lie on the minimum path. Further, the connectivity dimension, *c*, may be evaluated for symmetric stars from equation (12) as [28],

$$c = \frac{\ln z}{\left\{\ln z + \ln\left(\frac{2}{f}\right)\right\}} \tag{13}$$

A “meandering” mole fraction $\left(\phi_M\right)$ can be defined as the fraction that accounts for mass that is not used in direct or linear connectivity [28],

$$\phi_M = \frac{(z-s)}{z} = 1 - z^{-\left(1-\frac{1}{d_{\min}}\right)} \tag{14}$$

As the functionality, f, increases, $d_{\min}$ and ϕ_M are expected to decrease since steric constraints on the chain conformation increase in comparison to linear chains. For linear chains in the absence of steric effects, ideal scaling behavior is expected. For a good solvent, $d_{\min} \approx 5/3$. Steric interactions between arms in a star have the effect of extending the star arms towards, $d_{\min} \to 1$, for a fully extended chain. The limits of an unperturbed (linear) chain and a fully extended chain can be used to define a measure of steric interaction between the arms of a star as [28, 35],

$$\phi_{Si} = \frac{\langle \Delta s \rangle_f}{\langle \Delta s \rangle_\infty} = \frac{s_f - s_{linear}}{s_\infty - s_{linear}} = \frac{z^{\frac{1}{d_{\min}}} - z^{\frac{1}{d_{f,l}}}}{z - z^{\frac{1}{d_{f,l}}}} \tag{15}$$

where $d_{f,l}$ is the fractal dimension of an unperturbed arm under the given solvation conditions [28] and therefore, $d_{f,l} \sim 5/3$ under good-solvent conditions, and 2 under theta solvent conditions. ϕ_{Si} is an unique quantitative measure of steric effects in stars (extendible to any branched structure). For star polymers, ϕ_{Si} is the fraction of the extra extension, $\langle \Delta s \rangle_f$, in an arm induced due to presence of other connected arms in the chain, to that of the maximum possible extension under $f \to \infty$ condition, $\langle \Delta s \rangle_\infty$. It provides a quantitative measure of the extension of an arm induced due to presence of other arms in the chain. In absence of other branches, *i.e.* for linears, ϕ_{Si} is zero while it is maximum at 1, for a star with straight arms.

Scattering Functions for Star Polymers:

Small-angle scattering can be used to quantify the scaling model parameters [28, 31, 36-38]. For macromolecules in dilute solution, contrast enhancement is often achieved by examining hydrogen polymers in deuterated solvents using neutron scattering (SANS).

In order to examine stars under good solvent conditions, a fractal model by Teixeira *et al.* [39], has been employed [40], which is based on the pair correlation function [41],

$$g(r) \sim r^{d_f-3} e^{-r/\xi} \tag{16}$$

This pair correlation function takes advantage of the simple Fourier transform of a fractal scattering power law for the first term. The problem with this transform is that it reaches infinity at $r=0$ making the inverse transform impossible. Since there is no basis to "cut-off" the power-law term at low r, an ad hoc approach is introduced. In equation (2), r is the distance between chain units, d_f is the fractal dimension and ξ is defined as the fractal correlation length which is an artificially introduced size scale for the ad hoc exponential 'cutoff' term in equation (16). This exponential term was proposed by Debye and Bueche when they observed the scattering profile of blue light by Lucite [42]. Debye and Bueche treated $g(r)$ in a similar way to Debye's charge screening function parameterized by the screening length. They introduced an exponential cut-off function as an "example" after defining ξ as a "kind" of correlation length, in direct analogy to a screening length [42]. Equation (16) is used to obtain the scattered intensity given by Teixeira *et al.* [39],

$$I(q)=1+\frac{1}{(qR_m)^{d_f}}\frac{d_f\Gamma(d_f-1)}{\left\{1+(q\xi)^{-2}\right\}^{\frac{(d_f-1)}{2}}}\sin\left\{(d_f-1)\tan^{-1}(q\xi)\right\} \tag{17}$$

where, $q=\frac{4\pi}{\lambda}\sin\left(\frac{\theta}{2}\right)$, is the scattering wave vector for a radiation of wavelength λ and R_m is the mean radius of the particle. Equations (16) and (17) are based on the ad hoc exponential cutoff term, $e^{-r/\xi}$, that was an empirical proposition of Debye and Bueche [42]. The exponential function has no connection to physical structure and the length scale ξ lacks physical meaning.

Benoit evaluated intensity for a star poymer with f arms by modifying Debye's scattering function for a Gaussian polymer chain to account for inter-arm interactions [43-45],

$$\left\langle I(q)\right\rangle\approx\frac{2}{fx^2}\left[\left\{x-\left(1-e^{-x}\right)\right\}+\frac{f-1}{2}\left\{\left(1-e^{-x}\right)^2\right\}\right] \tag{18}$$

with, $x=\frac{f}{3f-2}q^2\left\langle R^2_{g_{arm}}\right\rangle$ where, $\left\langle R^2_{g_{arm}}\right\rangle$ is the Gaussian mean squared radius of gyration of an arm. Equation (18) includes two terms in the main bracket, the first of which reflects scattering from the f arms as individual Gaussian chains, $I_1(q)\approx\frac{2}{x^2}\left\{x-\left(1-e^{-x}\right)\right\}$ and is similar to Debye's scattering function for linear chains. This term dominates the scattering at very high-q. The second term in the main bracket, $I_2(q)\approx\frac{f-1}{fx^2}\left\{\left(1-e^{-x}\right)^2\right\}$, reflects interference between chain units on different arms of the star polymer and dominates the scattering at intermediate and low-q but imparts negligible contribution to the scattered intensity at high-q. Therefore equation (18) predicts a slope of -2 at high-q associated with a Gaussian chain. This is consistent with the modification of the Flory-Krigbaum theory presented above for star polymers and the Zimm-Stockmayer prediction for star size. The Beniot model is a fractal model with constant chain scaling, that is, it does not agree with the DC model. For Gaussian stars the Benoit model has been widely used to model scattering data.

Hybrid Unified Fit Function

Generally, SANS data from a dilute polymer solution displays two structural levels [28, 32, 35]. In each structural level, a Guinier's law, $I(q) \sim G\exp\left(-q^2R_g^2/3\right)$, and a power-law, $I(q) \sim B_f q^{-d_f}$, are observed at lower and higher q-values respectively, where G, R_g, B_f and d_f are the Guinier's law prefactor, radius of gyration, power-law prefactor and fractal dimension $\left(1 \le d_f \le 3\right)$ respectively. Together, these laws give an account of local features like size (R_g and persistent length, $l_p = l_k/2$) and mass fractal dimension. However, in star polymers, owing to the common branch point for the arms, Benoit found that another set of Guinier and power laws are induced due to inter-arm interactions [45]. This has been experimentally demonstrated. In addition to these structural parameters, the Flory interaction parameter, χ, can be quantified using the random phase approximation, RPA, equation, accounting for the enthalpy of mixing for a polymer in solution. Taking account these interactions in the star polymer under dilute solvent conditions, Rai obtained [28],

$$\frac{1}{I(q)}=\frac{1}{G_f}\left(\left[\begin{array}{l}\frac{f-1}{2}\left\{e^{-(qR_g)^2/3}+\frac{d_{\min}^2\Gamma\left(d_f-1\right)}{R_g^{2d_f}}e^{-(ql_p)^2/9}\left(q_f^*\right)^{-2d_f}\right\}\\+\left\{e^{-(qR_g)^2/3}+K_f e^{-(ql_p)^2/9}\left(q_f^*\right)^{-d_f}\right\}+\frac{1}{z}\left\{e^{-(ql_p)^2/9}+zK_p\left(q_p^*\right)^{-1}\right\}\end{array}\right]^{-1}+z\phi K_v\left(1-\frac{2\chi}{\sqrt{K_v}}\right)\right)$$

(19)

where, Γ is the gamma function, $q_i^*=q\Big/\left\{erf\left(qk_{sc}R_{g,i}\big/\sqrt{6}\right)\right\}^3$, $k_{sc}\approx 1.06$, and *erf* is the error function [33, 34]. Equation (19) has three structural levels in the square bracket along with a term outside of the square brackets that accounts for the enthalpy of mixing. χ is the Flory-Huggins' interaction parameter per Kuhn unit and is based on the zero conformational entropy units, the Kuhn units, rather than the chemical mer units, ϕ is the polymer volume fraction and $K_v=\frac{v_{pol}}{v_{sol}}$, where, v_{pol} and v_{sol} are the segmental volume of the Kuhn unit and the solvent molecule respectively. Amongst the three pairs of structural terms in the square brackets, the first term with lead factor of $\left(f-1\right)/2$ accounts for the inter-arm interactions similar to Benoit's second term in equation (18). The second term accounts for scattering from the star in the absence of correlations between arms while the third term with subscript p represent the rod-like persistent scaling regime. In each bracket, the first term represents the Guinier's exponential decay and the second term yields the power-law. $z=G_f/G_p$, is the weight average number of Kuhn units in the star molecule [31]. K_f and K_p are ratios of power-law prefactor to Guinier prefactor for fractal and persistent regimes. l_p and R_g are the persistent length and the radius of gyration of the fractal star polymer respectively [32]. It is assumed here that the Kuhn length, $l_k = 2l_p$ is the zero entropy unit [29] for the star. The Guinier prefactor for the fractal regime, G_f is given by [28],

$$G_f = v_{pol} z \phi N_A \left(b_{pol} - b_{sol}\right)^2 \tag{20}$$

where, and b_{pol} and b_{sol} are the scattering length densities of polymer Kuhn unit and solvent molecule respectively [28, 46]. $d_{\min}$ for a monodisperse star is given by [28, 31, 32, 47],

$$d_{\min} = \frac{B_f R_g^{d_f}}{G_f \Gamma\left(\frac{d_f}{2}\right)} \tag{21}$$

Equation (21) is valid for monodisperse samples [32, 47]. The second virial coefficient (A_2) is related to the Flory's χ-parameter by, [28]

$$A_2 = \frac{\left(\frac{1}{2} - \chi\right)}{V_{pol} \rho_{pol}^2} \tag{22}$$

where, V_{pol} and ρ_{pol} are the molar volume of the solvent and the density of polymer respectively.

MATERIAL AND METHODS

Small-angle neutron scattering (SANS) was performed on one weight percent solutions of polyisoprene stars in deuterated *p*-xylene at 34.5 ˚C. Deuterated p-xylene was purchased from Cambridge Isotopes. A small amount of 500 ppm of butylhydroxytoluene was added as a stabilizer before addition of polymer. It was experimentally determined that the solutions were below the overlap concentration.

SANS experiments were carried out at the HFIR CG-2 General-Purpose SANS facility at Oak Ridge National Laboratory (ORNL) and at the NCNR NG7 SANS facility at the National Institute of Standards and Technology (NIST). At CG-2, SANS experiments were run at sample to detector distances of 18.5 and 0.75 m, while at NG7, experiments were done at 15, 7 and 1m. The low-*q* data was calibrated with aluminum standard to obtain absolute intensity.

Two linear standards were purchased from PSS Polymer Standards Service GmbH, Mainz, Germany with M_w of (i) 23.6 kg/mole, M_n of 23.3 kg/mole, PDI of 1.01 and (ii) 85.4 kg/mole, M_n of 84.2 kg/mole, PDI of 1.01. Other linear, three arm, four-arm and six-arm polyisoprene stars were synthesized by anionic polymerization utilizing high vacuum techniques and standard chlorosilane chemistry [48]. In brief, all polymerizations and linking reactions were carried out in evacuated, *n*-BuLi-washed, and solvent-rinsed glass reactors. Reagents were introduced via break-seals and aliquots for characterization were removed by heat-sealing of constrictions. Firstly, narrow molecular weight linear living polyisoprenes were prepared, with *sec*-BuLi as initiator, in benzene at 25 ˚C. A small aliquot of the living PI was removed, terminated with degassed MeOH, and used for molecular weight characterization (arm of the star). The living polyisoprenyllithium, prior to reaction with the multifunctional chlorosilane compound, was end-capped with a few butadiene (Bd) units, in order to increase the living site reactivity. Trichloromethyl silane (CH_3SiCl_3), tetrachlorosilane ($SiCl_4$) and 1,2-bis(trichlorosilyl)-ethane (6-SiCl) were used as coupling agents for the synthesis of 3, 4 and 6-arm star PIs respectively. About 10% excess of the living end-capped PI to the SiCl, was used in order to force the linking reaction to completion. The excess living chains were terminated with degassed methanol and the final products (star + excess arm) were extensively fractionated (solvent/non-solvent: toluene/methanol) to remove the arm chains [48].

All intermediates and final products were analyzed by SEC and nuclear magnetic resonance (NMR). Size exclusion chromatography (SEC) experiments were carried out at 25 ˚C with a Waters model 510 pump, a Waters model 410 differential refractometer, and three Styragel columns having a porosity range from 10^3 to 10^6 Å. The carrier solvent was a mixture of chloroform/triethylamine (95/5, v/v) at a flow rate of 1.0 mL/min. Polystyrene standards were used for calibration, the M_n was obtained after applying appropriate correction coefficients. For all arms and stars the polydispersity index was lower than 1.1. The details for samples are givin in table 2. NMR spectra, generated with a Bruker 400-MHz instrument in $CDCl_3$ at 25 ˚C, revealed that all PIs have a high 1,4-content (93-94 %).

RESULTS AND DISCUSSION

The distinguishing feature of the SANS data on all samples is a power-law decay of close to -5/3 slope reflecting a mass fractal dimension of 5/3 following the prediction of equation (8), as shown in figure 2. In addition to this feature a prominent knee is observed at low-*q* reflecting correlations between the star arms. The effect of arm length can be seen in figure 2(b) where the knee shifts towards lower-*q* for higher arm molecular weights. Equation (19) was used to fit the experimental curves for the star samples listed in table 2, also shown for 4-arm stars in figure 2(b). The fitting and evaluated scaling parameters from the hybrid Unified fit are tabulated in table 3.

For constant arm length, both z as well as R_g increase with increase in functionality, as shown in figure 3(a) and (b). The persistence length, l_p, varies in the range of ~12.5±1.5 Å except for the linear sample for the 38k series. z, R_g and l_p all are somewhat higher for this sample.

The χ-parameter was constant within error limits at ~0.22±0.04, shown in figure 4(a). This agrees rather well with the reported values of 0.27 in literature [49, 50]. It should be pointed out that the χ-parameter evaluated here is based on the zero entropy Kuhn unit rather than the chemical mer unit. The second virial coefficient, A_2, shown in figure 4(b), has a value of ~0.0026±0.0004 $molcm^3/g^2$. None of these local enthalpic parameters are affected by functionality or molecular weight of the star polymers.

The data shows a rather constant fractal dimension, d_f, close to 5/3 across all sets of samples, figure 5(a), consistent with equation (8). The natural tendency for the structures to equilibrate to $d_f = 5/3$ is remarkable, supporting the modified Flory-Krigbaum prediction. The connectivity dimension, c, shown in figure 5(b), is bound by equation (12) to the functionality, f and z. Therefore differences between the three sets of samples with the same functionality reflect the effect of mass alone. Figure 5(b) also shows that c is high for short armed stars which is consistent with equation (13). $d_{\min}$, figure 5(c), is a conjugate parameter reflecting the average tortuosity in the structure. The decrease in tortuosity with functionality indicates that the arms straighten out as functionality increases, maintaining a constant mass fractal dimension. As c is high for short-armed stars, $d_{\min}$ actually decreases since the overall mass density remains constant.

It essentially means that at an average, the arms of stars with higher mass are comparatively more tortuous.

The minimum path, p, is the number of Kuhn units from one side of the star to the other, so two arm lengths, figure 6(a). This remains constant with functionality for a fixed arm mass, as anticipated. The connective path, s quantifies the mass of a stick figure structure connecting end points and the core in terms of number of Kuhn units, shown in figure 6(b). Normalizing by the number of arms, s/f, it can be clearly seen that the arms straighten out with increasing functionality, shown in figure 6(c). s increases with functionality due to straightening of the arms. s also increases with mass of the arms. The meandering mole fraction, ϕ_M, which is the fraction of chain that accounts for mass that is not used in linear (stick figure) connectivity can be evaluated using equation (9). ϕ_M decreases with increase in functionality, shown in figure 6(d), indicating that the arms are less convoluted with increasing functionality.

The monomer density of the chain is a function of the mass, $\rho = z^{1-1/d_f}$. The stars display constant mass fractal dimension according to equation (8). Since the mass fractal dimension is constant, there is no significant change in local density as a function of radial position in the star as was predicted by the D&C model. Rather, the stars behave similar to the Benoit fractal model, but with good-solvent scaling. The radially varying feature of the star structure is an increase in chain tortuosity with distance from the core rather than the density gradient assumed in the D&C model. The radial increase in tortuosity allows for a constant radial density profile.

The scaling parameters consistently point toward straightening of the arms with functionality, shown in figure 5. The local mass density, reflected in the mass-fractal dimension, remains the same, Figure 5(a), while the minimum dimension decays with functionality indicating a reduction in tortuosity with functionality. Such a steric phenomenon can be quantified using equation (15). ϕ_{Si} is a mole fraction quantifying steric effects, shown in figure 7(a). Steric effects are greater at higher functionalities and lower arm molecular weights. ϕ_{Si} for the 6-arm stars rise to 0.36±0.06, 0.181±0.007 and 0.135±0.004 for 10.5k, 38k, and 46k-arm stars respectively. The corresponding ϕ_{Si} for 4-arm stars are 0.17±0.02, 0.101±0.001, and 0.085±0.005 and that for 3-arm stars are 0.104±0.006, 0.059±0.003 and 0.049±0.002. ϕ_{Si} for the six arm 10.5k sample is about 36% of a fully extended arm structure!

Figure 8 is a schematic, projected in 2D for clarity, summarizing the scaling parameters considered in the present investigation. The local mass density of the structure remains radially the same. In order to accommodate an increase in conical volume with radius the chain becomes more tortuous. The results may be compared and contrasted with the Daoud & Cotton (D&C) model where the local density is predicted to decrease with radial position away from the center. The D&C model predicts three regimes based on relationships between density, f and z. In contrast, the modified Flory-Krigbam approach and results shown here predict that the density is given by $\phi(r) \sim (r/l)^{-4/3}$ irrespective of distance from core.

CONCLUSION

Molecular topology generally has a direct influence on the mass fractal dimension and other scaling dimensions for fractal structures. In this paper it is shown that polymers at thermal equilibrium are a distinct class of fractals where the mass-fractal dimension is not affected by chain topology. The consequence of this is chain straightening with increasing chain complexity. A theoretical basis for this observation comes from a slight modification to the Flory-Krigbaum theory.

The chain scaling dimensions and interaction parameter of star topologies was obtained using a hybrid Unified scattering function that accounts for inter-arm correlations in symmetric star polymers along with the polymer-solvent interaction parameter for chains of arbitrary scaling dimension. The structural and thermodynamic parameters for different molecular weights and functionality polyisoprene stars were considered under good solvent conditions.

The results were compared and contrasted with the Daoud & Cotton (D&C) model where equal segments of the arms are confined to blobs of radially increasing size, which can fit within a cone, leading to a radially decreasing chain density. Our results contradicted the presumption that a radial density gradient exists. The results demonstrate the ability of star topologies to redistribute the mass through changes in chain tortuosity such that the mass fractal dimension remains constant throughout the structure and for stars of different functionality.

For symmetric star polymers the branch fraction, ϕ_{Br}, can be directly calculated from the star functionality, leading to a verification of the structure. Our results quantify steric effects in symmetric stars and show that steric straightening in star polymers is more significant for lower molecular weight arms and stars with higher functionalities. A modification of the Flory and Krigbaum theory showed that the size of stars depends on the mass, functionality and Kuhn length with a similar dependence to that of the D&C model except that the dependence on Kuhn length is slightly different.

ACKNOWLEDGEMTS

The research conducted at ORNL's High Flux Isotope Reactor was sponsored by the Scientific User Facilities Division, Office of Basic Energy Sciences, U.S. Department of Energy (USA). We acknowledge the support of the National Institute of Standards and Technology (USA), U.S. Department of Commerce, in providing the neutron research facilities used in this work. RK and NH thank Dr Ema Zagar, National Institute of Chemistry Slovenia, for the SEC-MALS characterization of the star PIs. DKR is supported by the Laboratory Directed Research and Development program of Oak Ridge National Laboratory.

REFERENCES

[1] J. R. Schaefgen and P. J. Flory, Synthesis of multichain polymers and investigation of their viscosities, Journal of the American Chemical Society **70**, 2709 (1948).

[2] J. M. Desimone, Branching out into new polymer markets, Science **269**, 1060 (1995).

[3] C. Mayer, E. Zaccarelli, E. Stiakakis, C. N. Likos, F. Sciortino, A. Munam, M. Gauthier, N. Hadjichristidis, H. Iatrou, P. Tartaglia, H. Lowen and D. Vlassopoulos, Asymmetric caging in soft colloidal mixtures, Nature Materials **7**, 780 (2008).

[4] M. Watzlawek, C. N. Likos and H. Lowen, Phase diagram of star polymer solutions, Physical Review Letters **82**, 5289 (1999).

[5] G. Widawski, M. Rawiso and B. Francois, Self-organized honeycomb morphology of star-polymer polystyrene films, Nature **369**, 387 (1994).

[6] D. K. Bick and T. C. B. McLeish, Topological contributions to nonlinear elasticity in branched polymers, Physical Review Letters **76**, 2587 (1996).

[7] S. T. Milner and T. C. B. McLeish, Reptation and contour-length fluctuations in melts of linear polymers, Physical Review Letters **81**, 725 (1998).

[8] N. Hadjichristidis, M. Pitsikalis, S. Pispas and H. Iatrou, Polymers with complex architecture by living anionic polymerization, Chemical Reviews **101**, 3747 (2001).

[9] J. Batoulis and K. Kremer, Thermodynamic properties of star polymers - good solvents, Macromolecules **22**, 4277 (1989).

[10] J. Roovers, P. M. Toporowski and J. Douglas, Thermodynamic properties of dilute and semidilute solutions of regular star polymers, Macromolecules **28**, 7064 (1995).

[11] B. H. Zimm and W. H. Stockmayer, The dimensions of chain molecules containing branches and rings, The Journal of Chemical Physics **17**, 1301 (1949).

[12] G. S. Grest, L. J. Fetters, J. S. Huang and D. Richter, in Advances in chemical physics, vol xciv, 1996), Vol. 94, p. 67.

[13] M. Daoud and J. P. Cotton, Star shaped polymers - a model for the conformation and its concentration-dependence, Journal De Physique **43**, 531 (1982).

[14] T. M. Birshtein and E. B. Zhulina, Conformations of star-branched macromolecules, Polymer **25**, 1453 (1984).

[15] W. D. Dozier, J. S. Huang and L. J. Fetters, Colloidal nature of star polymer dilute and semidilute solutions, Macromolecules **24**, 2810 (1991).

[16] P. M. Wood-Adams, J. M. Dealy, A. W. deGroot and O. D. Redwine, Effect of molecular structure on the linear viscoelastic behavior of polyethylene, Macromolecules **33**, 7489 (2000).

[17] R. Everaers, S. K. Sukumaran, G. S. Grest, C. Svaneborg, A. Sivasubramanian and K. Kremer, Rheology and microscopic topology of entangled polymeric liquids, Science **303**, 823 (2004).

[18] L. J. Fetters, A. D. Kiss, D. S. Pearson, G. F. Quack and F. J. Vitus, Rheological behavior of star-shaped polymers, Macromolecules **26**, 647 (1993).

[19] A. T. Boothroyd and R. C. Ball, Conformation of star polymers without excluded volume, Macromolecules **23**, 1729 (1990).

[20] P. G. De Gennes, *Scaling concepts in polymer physics* (Cornell University Press, New York, 1979).

[21] H. Benoit, On the effect of branching and polydispersity on the angular distribution of the light scattered by gaussian coils, Journal of Polymer Science **11**, 507 (1953).

[22] J. S. Pedersen, in 3rd European Summer School on Scattering Methods Applied to Soft Condensed Matter, Bombannes, France, 1997), p. 171.

[23] F. Candau, P. Rempp and H. Benoit, A new theoretical approach to the problem of solution behavior of branched polymers, Macromolecules **5**, 627 (1972).

[24] T. A. Orofino, Branched polymers. Ii—dimensions in non-interacting media, Polymer **2**, 305 (1961).

[25] P. J. Flory and J. G. Jackson, *Statistical mechanics of chain molecules* (Hanser, 1989).

[26] W. R. Krigbaum and P. J. Flory, Statistical mechanics of dilute polymer solutions .3. Ternary mixtures of 2 polymers and a solvent, Journal of Chemical Physics **20**, 873 (1952).

[27] W. R. Krigbaum and P. J. Flory, Statistical mechanics of dilute polymer solutions. V. Evaluation of thermodynamic interaction parameters from dilute solution measurements1, Journal of the American Chemical Society **75**, 5254 (1953).

[28] D. K. Rai, G. Beaucage, K. Ratkanthwar, P. Beaucage, R. Ramachandran and N. Hadjichristidis, Determination of the interaction parameter and topological scaling features of symmetric star polymers in dilute solution, Physical Review E **92**, 012602 (2015).

[29] W. Kuhn, Über die gestalt fadenförmiger moleküle in lösungen, Kolloid-Zeitschrift **68**, 2 (1934).

[30] G. Beaucage and A. S. Kulkarni, Dimensional description of cyclic macromolecules, Macromolecules **43**, 532 (2010).

[31] G. Beaucage, Determination of branch fraction and minimum dimension of mass-fractal aggregates, Physical Review E **70**, 031401 (2004).

[32] R. Ramachandran, G. Beaucage, A. S. Kulkarni, D. McFaddin, J. Merrick-Mack and V. Galiatsatos, Persistence length of short-chain branched polyethylene, Macromolecules **41**, 9802 (2008).

[33] G. Beaucage, Approximations leading to a unified exponential power-law approach to small-angle scattering, Journal of Applied Crystallography **28**, 717 (1995).

[34] G. Beaucage, Small-angle scattering from polymeric mass fractals of arbitrary mass-fractal dimension, Journal of Applied Crystallography **29**, 134 (1996).

[35] R. Ramachandran, G. Beaucage, D. K. Rai, D. J. Lohse, T. Sun, A. H. Tsou, A. Norman and N. Hadjichristidis, Quantification of branching in model three-arm star polyethylene, Macromolecules **45**, 1056 (2012).

[36] D. K. Rai, G. Beaucage, E. O. Jonah, D. T. Britton, S. Sukumaran, S. Chopra, G. G. Gonfa and M. Harting, Quantitative investigations of aggregate systems, The Journal of Chemical Physics **137**, 044311 (2012).

[37] D. K. Rai, Quantification of Fractal Systems using Small Angle Scattering, Doctoral dissertation, University of Cincinnati, 2013.

[38] D. Anunciado, D. Rai, S. Qian, V. Urban and H. O'Neill, Small-angle neutron scattering reveals the assembly of alpha-synuclein in lipid membranes, Biochimica et Biophysica Acta (BBA) - Proteins and Proteomics **1854**, 1881 (2015).

[39] J. Teixeira, Small-angle scattering by fractal systems, Journal of Applied Crystallography **21**, 781 (1988).

[40] U. S. Jeng, T. L. Lin, L. Y. Wang, L. Y. Chiang, D. L. Ho and C. C. Han, Sans structural characterization of fullerenol-derived star polymers in solutions, Appl. Phys. A-Mater. Sci. Process. **74**, S487 (2002).

[41] S. K. Sinha, Freltoft, T. and J. Kjems, in Kinetics of aggregation and gelation, edited by F. Family and D. P. Landau (North-Holland, Amsterdam, 1984), p. 87.

[42] P. Debye and A. M. Bueche, Scattering by an inhomogeneous solid, Journal of Applied Physics **20**, 518 (1949).

[43] A. T. Boothroyd, G. L. Squires, L. J. Fetters, A. R. Rennie, J. C. Horton and A. Devallera, Small-angle neutron-scattering from star-branched polymers in dilute-solution, Macromolecules **22**, 3130 (1989).

[44] J. S. Pedersen, Analysis of small-angle scattering data from colloids and polymer solutions: Modeling and least-squares fitting, Advances in Colloid and Interface Science **70**, 171 (1997).

[45] H. Benoit, On the effect of branching and polydispersity on the angular distribution of the light scattered by gaussian coils, J. Polym. Sci. **11**, 507 (1953).

[46] G. Beaucage and R. S. Stein, Tacticity effects on polymer blend miscibility. 3. Neutron scattering analysis, Macromolecules **26**, 1617 (1993).

[47] R. Ramachandran, G. Beaucage, A. S. Kulkarni, D. McFaddin, J. Merrick-Mack and V. Galiatsatos, Branch content of metallocene polyethylene, Macromolecules **42**, 4746 (2009).

[48] N. Hadjichristidis, H. Iatrou, S. Pispas and M. Pitsikalis, Anionic polymerization: High vacuum techniques, Journal of Polymer Science Part a-Polymer Chemistry **38**, 3211 (2000).

[49] Y. B. Tewari and H. P. Schreiber, Thermodynamic interactions in polymer systems by gas-liquid chromatography. Ii. Rubber-hydrocarbons, Macromolecules **5**, 329 (1972).

[50] J. E. Mark, *Physical properties of polymers* (Cambridge University Press, 2004).

Figures and Tables

Figure 1: Schematic of a six-arm PI star polymer of fractal dimension d_f *and composed of z Kuhn units of length* l_k*. The structure can be decomposed into two sets of conjugate parameters describing connectivity* (s,c) *and tortuosity* $(p,d_{\min})$*. The connective path is composed of* s *units and has its nascent fractal dimension called the connective dimension* c*; and describes the branching characteristics in chain is shown in straight black dashed lines. Any two branches of a symmetric star forms a minimum path across the whole structure composed of* p *Kuhn units with a nascent fractal dimension called minimum dimension of* $d_{\min}$*.* p *describe the average topological tortuosity and is shown in units with dark borders.*

Figure 2 (a) SANS data from ~1% by weight 38k-arm star polyisoprene polymer solution in xylene for linear, 3-arm, 4-arm and 6-arm in black, dark grey dots, grey dash-dot and light grey dashes respectively (b) SANS from solution of ~1% by weight for 4-arm star polyisoprene in xylene for 10.5k, 38k and 46k arms in black triangles, dark grey squares and light grey circles with respective with Hybrid Unified Fits {Eq (19)} in solid contrast lines. The data and their respective fits are offset for visual clarification. Slopes of -5/3 and -1 are also shown for reference.

Figure 3 (a) Mass z*, (b) radius of gyration,* R_g*, and (c) persistent lengths,* l_p*, as a function of functionality,* f*.*

Figure 4 (a) Flory-Huggins's interaction parameter, χ*, and (b) second virial coefficient,* A_2*, as a function of functionality,* f*.*

Figure 5 (a) fractal dimension, d_f*, (b) connectivity dimension, c, and (c) minimum dimension,* d_{min} *as a function of functionality,* f*.*

Figure 6 (a) minimum path, p*, (b) connectivity path,* s*, (c)* s/f*, and (d) meandering mole fraction* (ϕ_M) *as a function of functionality,* f*.*

Figure 7 (a) ϕ_{Si}*, and (b)* s/z *as a function of functionality,* f*.*

Figure 8 Schematic demonstrating changes in scaling and thermodynamic parameters with functionality for the same arm length. The scaling model for 6-arm is compared with that of Daoud-Cotton model [13]. l *and* ν *are monomer length and excluded volume associated with each monomer.*

Table 1. Summary of R *dependence on scaling parameters,* f*,* z*,* l_k *and* V_C*.*

Table 2. Synthesis and characterization details for linear, 3-arm, 4-arm and 6-arm PI star polymers each with an arm molecular weight of ~10.5, 38 and 46 kg/mole.

Table 3. Fitted, thermodynamic and calculated scaling parameters for PI polymer samples using the Unified Fit Function Eq. (19)

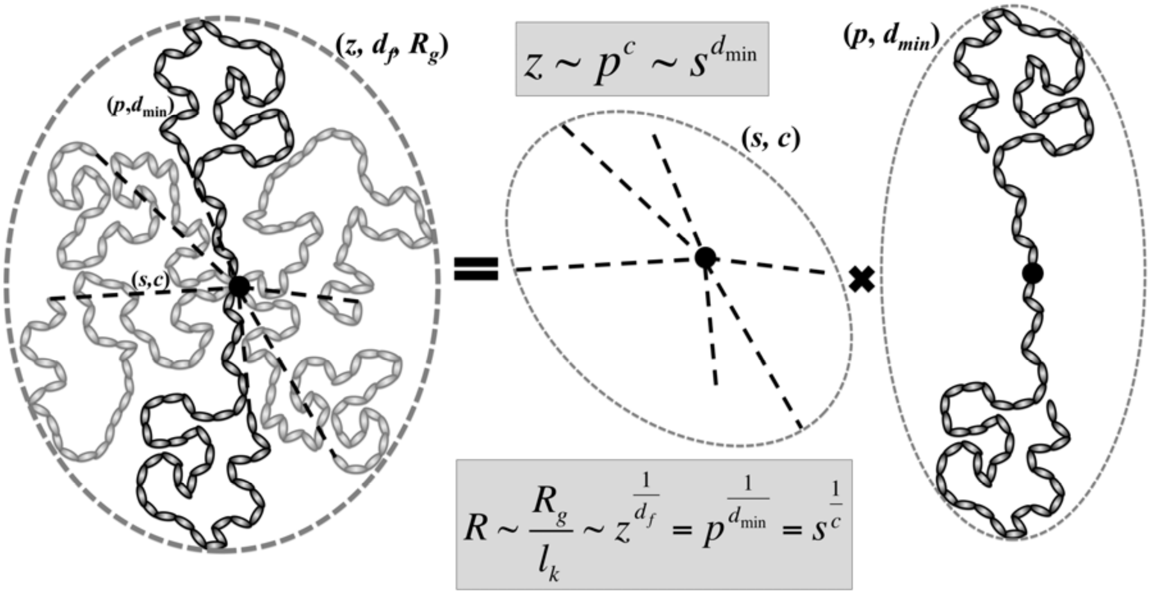
(z, d_f, R_g)
$(p, d_{\min})$
(s, c)
$z \sim p^c \sim s^{d_{\min}}$
(s, c)
(p, d_{min})
$R \sim \frac{R_g}{l_k} \sim z^{\frac{1}{d_f}} = p^{\frac{1}{d_{\min}}} = s^{\frac{1}{c}}$

Figure 1

z

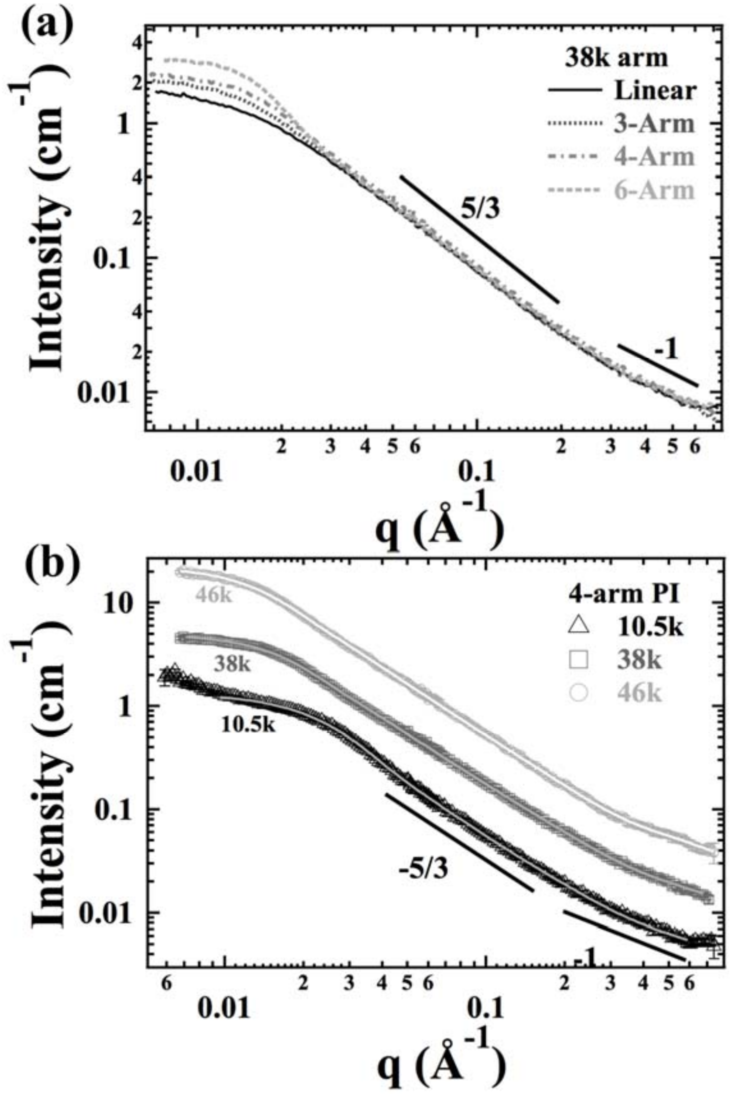
(a)
38k arm
Linear
3-Arm
4-Arm
6-Arm
5/3
-1
Intensity (cm^{-1})
4
2
1
4
2
0.1
4
2
0.01
0.01
2
3
4
5
6
0.1
2
3
4
5
6
q (Å^{-1})
(b)
4-arm PI
△ 10.5k
□ 38k
○ 46k
46k
38k
10.5k
-5/3
-1
Intensity (cm^{-1})
10
1
0.1
0.01
6
0.01
2
3
4
5
6
0.1
2
3
4
5
6
q (Å^{-1})

Figure 2

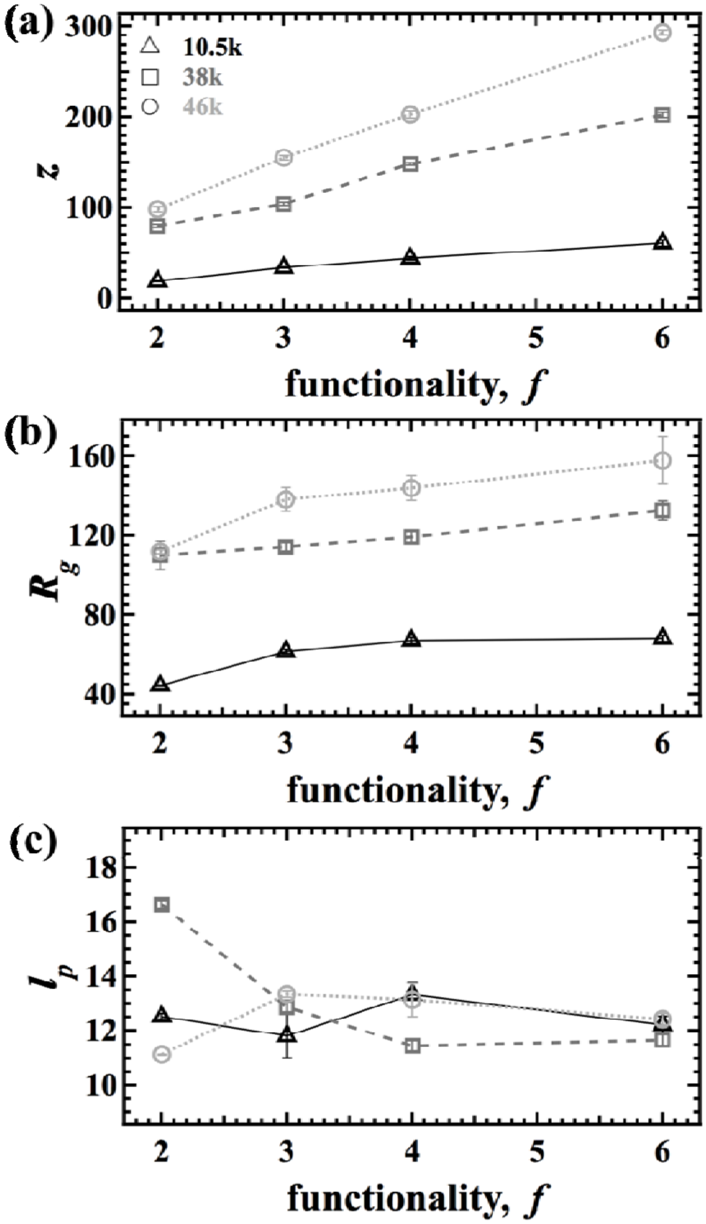
(a)
△ 10.5k
□ 38k
○ 46k
z
0
100
200
300
2
3
4
5
6
functionality, f
(b)
R_g
40
80
120
160
2
3
4
5
6
functionality, f
(c)
l_p
10
12
14
16
18
2
3
4
5
6
functionality, f

Figure 3

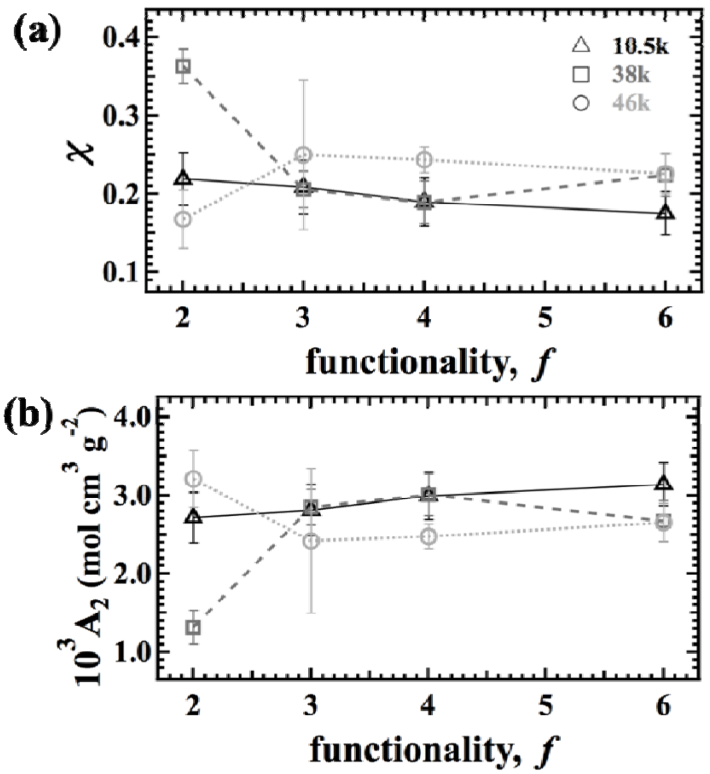
(a)
χ
0.4
0.3
0.2
0.1
△ 10.5k
□ 38k
○ 46k
2
3
4
5
6
functionality, f
(b)
$10^3 A_2$ (mol cm^3 g^{-2})
4.0
3.0
2.0
1.0
2
3
4
5
6
functionality, f

Figure 4

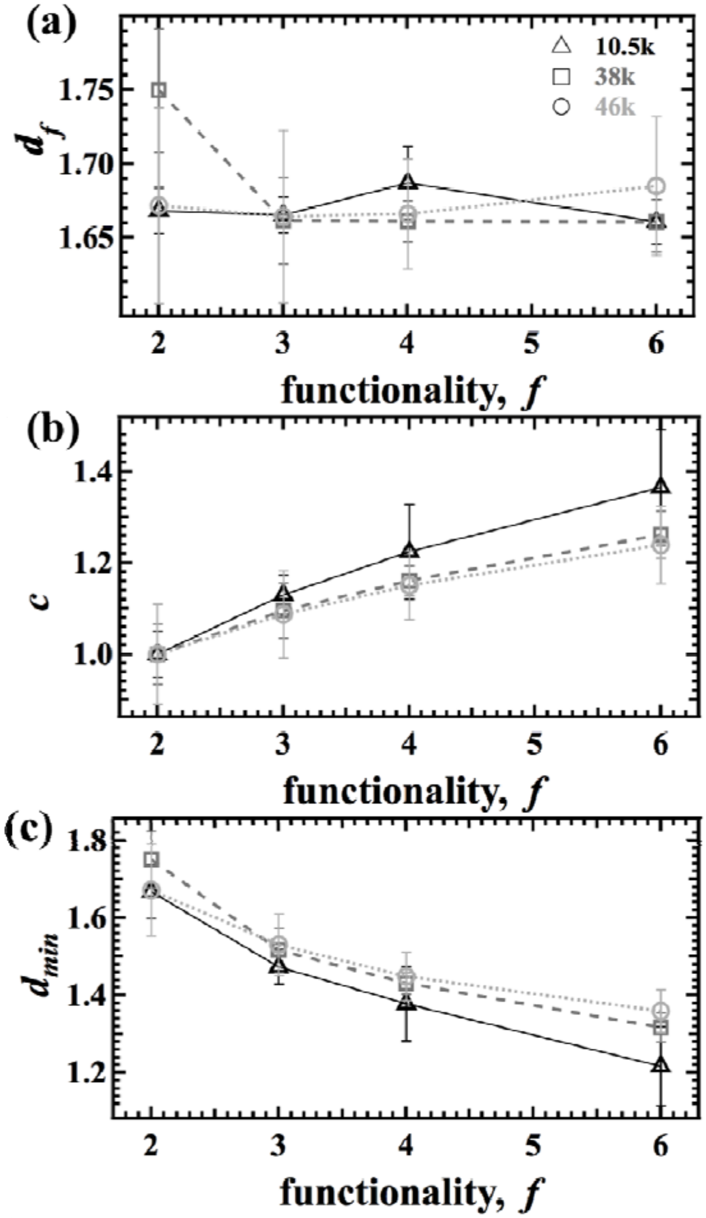
(a)
d_f
1.75
1.70
1.65
△ 10.5k
□ 38k
○ 46k
2
3
4
5
6
functionality, f
(b)
c
1.4
1.2
1.0
2
3
4
5
6
functionality, f
(c)
d_{min}
1.8
1.6
1.4
1.2
2
3
4
5
6
functionality, f

Figure 5

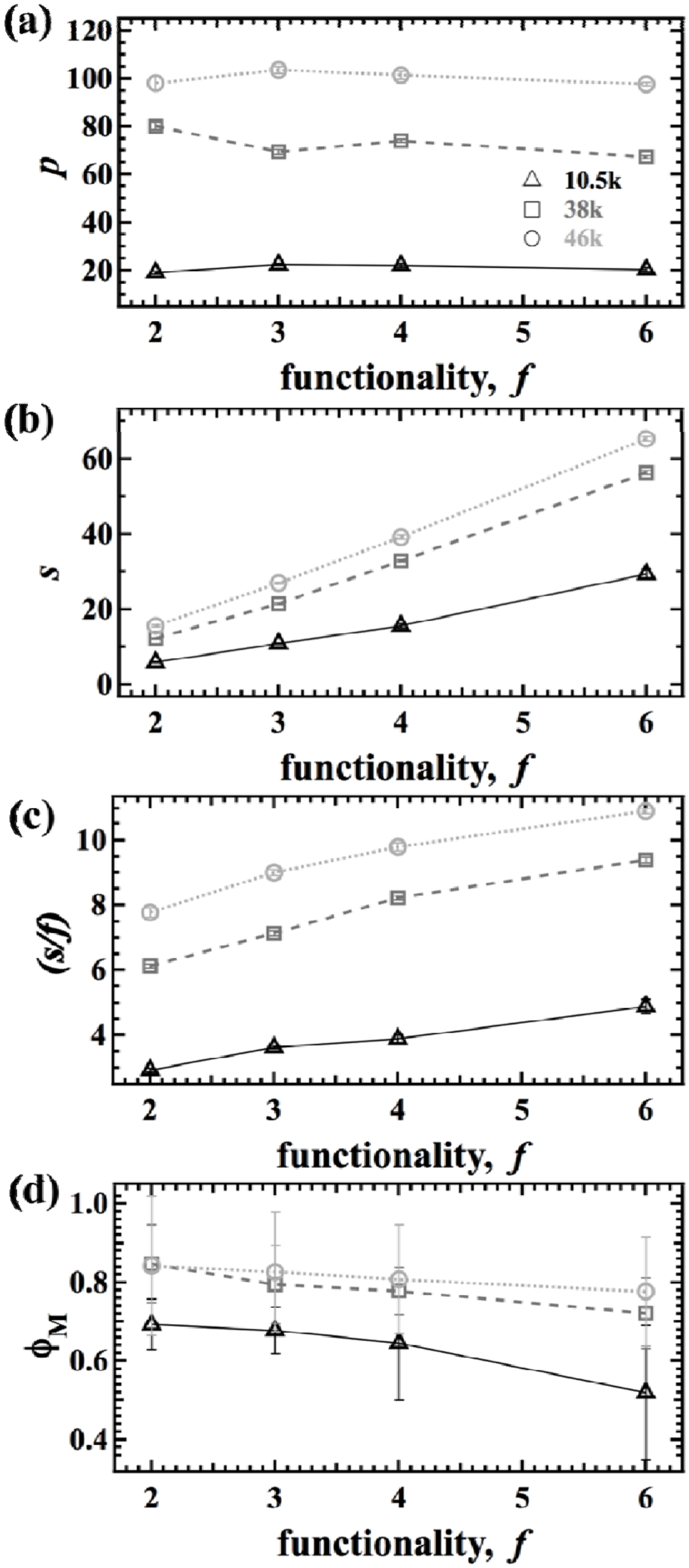
(a)
p
120
100
80
60
40
20
10.5k
38k
46k
2
3
4
5
6
functionality, f
(b)
s
60
40
20
0
2
3
4
5
6
functionality, f
(c)
(s/f)
10
8
6
4
2
3
4
5
6
functionality, f
(d)
ϕ_M
1.0
0.8
0.6
0.4
2
3
4
5
6
functionality, f

Figure 6

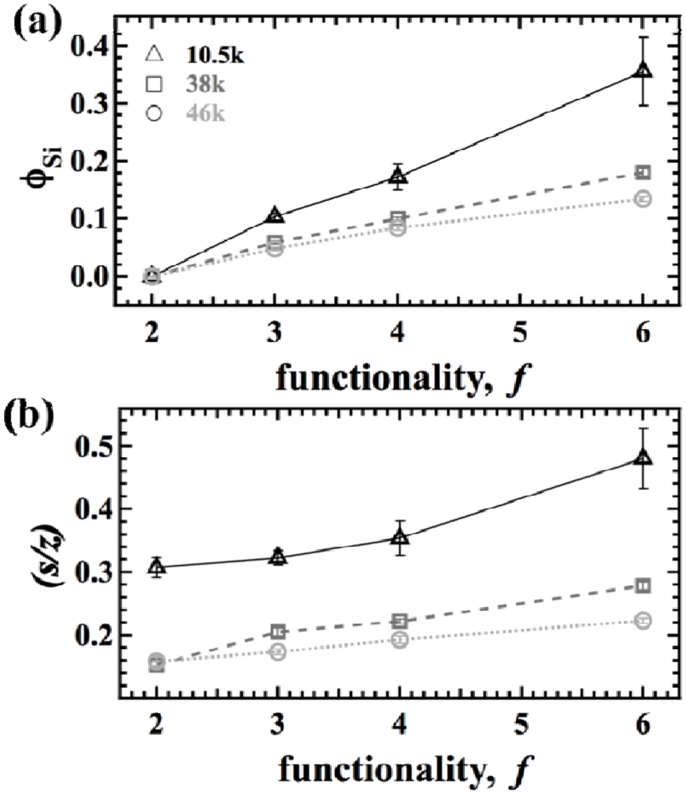
(a)
△ 10.5k
□ 38k
○ 46k
ϕ_Si
0.0
0.1
0.2
0.3
0.4
2
3
4
5
6
functionality, f
(b)
(s/z)
0.2
0.3
0.4
0.5
2
3
4
5
6
functionality, f

Figure 7

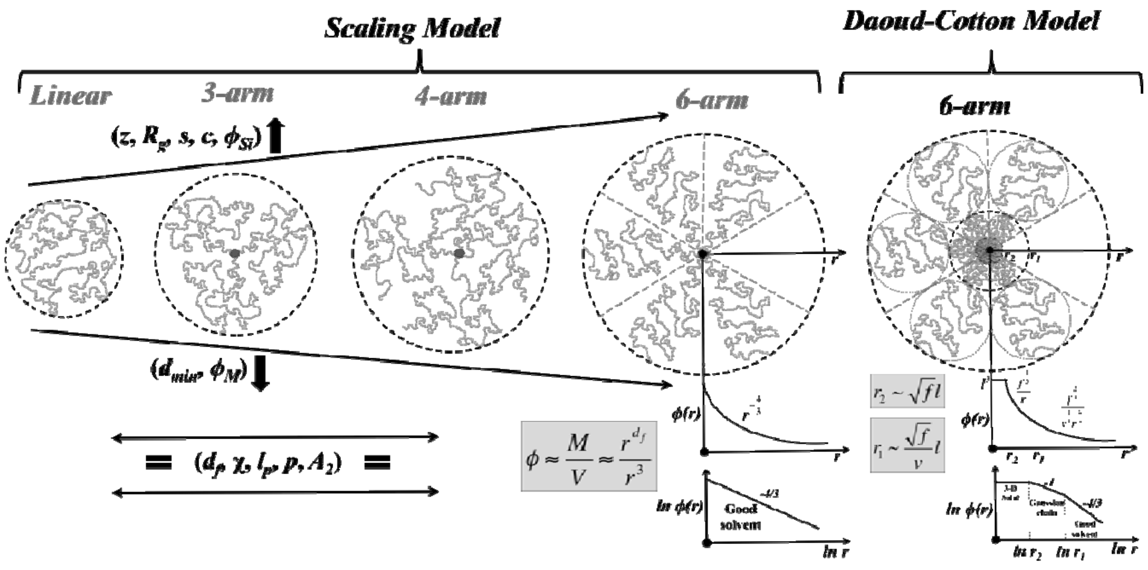
Scaling Model
Daoud-Cotton Model
Linear
3-arm
4-arm
6-arm
6-arm
$(z, R_g, s, c, \phi_{Si})$
(d_{min}, ϕ_M)
(d_f, χ, l_p, p, A_2)
$\phi \approx \frac{M}{V} \approx \frac{r^{d_f}}{r^3}$
$\phi(r)$
$r^{-\frac{4}{3}}$
r
$\ln \phi(r)$
-4/3
Good solvent
ln r
$r_2 \sim \sqrt{f}\, l$
$r_1 \sim \frac{\sqrt{f}}{v} l$
r_2
r_1
$\ln r_2$
$\ln r_1$

Figure 8

Table 1

Model	Theta Solvent	Good Solvent
Zimm Stockmeyer	$\frac{(3f-2)^{\frac{1}{2}}}{f} z^{\frac{1}{2}} l_k$	-
Daoud Cotton	$f^{-\frac{1}{4}} z^{\frac{1}{2}} l_k$	$f^{-\frac{2}{5}} z^{\frac{3}{5}} V_c^{\frac{1}{5}} l_k$
Modified Flory-Krigbaum	$\frac{(3f-2)^{\frac{1}{2}}}{f} z^{\frac{1}{2}} l_k$	$f^{-\frac{2}{5}} z^{\frac{3}{5}} V_C^{\frac{1}{5}} l_k^{\frac{2}{5}}$

Table 2

Arm	1,4-PI Type	M_n arm (kg/mol), SEC			Final star-branched PI (SEC-MALS)		$f = M_{n,star}/M_{n,arm}$	
		Cal.[a]	*SEC*[b]	M_w/M_n	M_n, kg/mol	M_w/M_n	*Cal.*[c]	*SEC*[d]
10.5k	Linear[a]	23.6	-	1.01	-	-	Linear	-
	3-arm	10	10.5	1.02	30.27	1.02	2.88	3.03
	4-arm	10	10.5	1.02	39.76	1.03	3.79	3.98
	6-arm	10	10.5	1.02	64.05	1.02	6.10	6.41
38k	Linear	74	68	1.01	68.13	1.02	Linear	-
	3-arm	35	38	1.03	101.0	1.01	2.66	2.89
	4-arm	35	38	1.03	133.2	1.01	3.51	1
	6-arm	35	38	1.03	201.4	1.01	5.30	5.75
46k	Linear[b]	85.4		1.01	-	-	Linear	-
	3-arm	50	46	1.01	132.7	1.03	2.88	2.65
	4-arm	50	46	1.01	181.7	1.01	3.95	3.63
	6-arm	50	46	1.01	267.7	1.01	5.82	5.35

[a] *Purchased from PSS Polymer Standards Service GmbH (Mw of 23.6 kg/mole, Mn of 23.3 kg/mole),* [b] *Purchased from PSS Polymer Standards Service GmbH (Mw of 85.4 kg/mole, Mn of 84.2 kg/mole),* [c] *Calculated values from chemical stoichiometry,* [d] *SEC/MALS determined values.*

Table 3

Arm MW	f	R_g $(\AA)$	z	d_f	χ^a	$10^3 A_2$ $(mol cm^3 g^{-2})$	l_p $(\AA)$	$d_{\min}$	c	p	s	ϕ_{Br}^b	ϕ_M	ϕ_{Si}
10.5k	*Linear*	*44.6 ±0.2*	*19 ±1*	*1.67 ±0.02*	*0.22 ±0.03*	*2.7 ±0.3*	*12.5 ±0.1*	*1.67 ±0.07*	*1.00 ±0.05*	*19.0 ±0.6*	*5.8 ±0.5*	*0.0 ±0.0*	*0.69 ±0.06*	*0.0 ±0.0*
	3	*62 ±1*	*34 ±1*	*1.67 ±0.01*	*0.21 ±0.03*	*2.8 ±0.3*	*11.8 ±0.8*	*1.47 ±0.04*	*1.13 ±0.04*	*22.5 ±0.4*	*11 ±1*	*0.33 ±0.05*	*0.67 ±0.08*	*0.104 ±0.006*
	4	*67 ±2*	*44 ±2*	*1.69 ±0.02*	*0.19 ±0.03*	*3.0 ±0.3*	*13.3 ±0.4*	*1.4 ±0.1*	*1.2 ±0.1*	*22.0 ±0.8*	*16 ±4*	*0.5 ±0.1*	*0.6 ±0.1*	*0.17 ±0.02*
	6	*68 ±2*	*61 ±4*	*1.66 ±0.01*	*0.18 ±0.03*	*3.1 ±0.3*	*12.2 ±0.3*	*1.2 ±0.1*	*1.4 ±0.1*	*20.4 ±0.8*	*30 ±10*	*0.7 ±0.2*	*0.5 ±0.2*	*0.36 ±0.06*
38k	*Linear*	*110 ±7*	*80 ±1*	*1.75 ±0.04*	*0.36 ±0.02*	*2.7 ±0.3*	*16.6 ±0.2*	*1.75 ±0.07*	*1.00 ±0.07*	*80 ±1*	*12.2 ±0.1*	*0.0 ±0.0*	*0.85 ±0.09*	*0.0 ±0.0*
	3	*114 ±2*	*104 ±2*	*1.66 ±0.02*	*0.20 ±0.02*	*2.8 ±0.3*	*12.9 ±0.2*	*1.52 ±0.06*	*1.10 ±0.06*	*69 ±1*	*21.4 ±0.3*	*0.33 ±0.08*	*0.79 ±0.09*	*0.059 ±0.003*
	4	*119 ±3*	*148 ±1*	*1.66 ±0.01*	*0.19 ±0.03*	*3.0 ±0.3*	*11.4 ±0.2*	*1.43 ±0.03*	*1.16 ±0.03*	*74.1 ±0.6*	*32.9 ±0.2*	*0.50 ±0.07*	*0.78 ±0.06*	*0.101 ±0.003*
	6	*133 ±5*	*202 ±3*	*1.66 ±0.02*	*0.22 ±0.03*	*3.1 ±0.3*	*11.7 ±0.2*	*1.32 ±0.04*	*1.26 ±0.05*	*67.4 ±0.7*	*56.3 ±0.6*	*0.7 ±0.1*	*0.72 ±0.09*	*0.181 ±0.007*
46k	*Linear*	*112 ±1*	*98 ±3*	*1.67 ±0.07*	*0.17 ±0.04*	*3.2 ±0.4*	*11.1 ±0.2*	*1.7 ±0.1*	*1.00 ±0.05*	*98 ±3*	*15.5 ±0.3*	*0.0 ±0.0*	*0.84 ±0.06*	*0.0 ±0.0*
	3	*138 ±6*	*155 ±2*	*1.66 ±0.06*	*0.25 ±0.09*	*2.4 ±0.9*	*13.4 ±0.1*	*1.53 ±0.08*	*1.09 ±0.09*	*104 ±2*	*27.0 ±0.3*	*0.3 ±0.1*	*0.83 ±0.08*	*0.049 ±0.002*
	4	*144 ±6*	*201 ±4*	*1.67 ±0.04*	*0.24 ±0.02*	*2.5 ±0.2*	*13.1 ±0.6*	*1.45 ±0.06*	*1.15 ±0.08*	*101 ±2*	*39.1 ±0.5*	*0.5 ±0.2*	*0.81 ±0.1*	*0.085 ±0.005*
	6	*160 ±10*	*293 ±3*	*1.68 ±0.05*	*0.23 ±0.03*	*2.7 ±0.2*	*12.4 ±0.2*	*1.36 ±0.06*	*1.24 ±0.09*	*98 ±1*	*65.3 ±0.5*	*0.7 ±0.2*	*0.78 ±0.2*	*0.135 ±0.004*

[a] *χ determined per Kuhn unit,* [b] *Bound by equation (8)*